Chemistry–A European Journal
Research Article
doi.org/10.1002/chem.202400411
Chemistry Europe
European Chemical Societies Publishing
www.chemeurj.org

Hot Paper

A Magnesium Binding Site And The Anomeric Effect Regulate The Abiotic Redox Chemistry Of Nicotinamide Nucleotides

Lorenzo Sebastianelli,[a] Harpreet Kaur,[a] Ziniu Chen,[a] Ramanarayanan Krishnamurthy,[b] and Sheref S. Mansy*[a]

Nicotinamide adenine dinucleotide (NAD^+) is a redox active molecule that is universally found in biology. Despite the importance and simplicity of this molecule, few reports exist that investigate which molecular features are important for the activity of this ribodinucleotide. By exploiting the nonenzymatic reduction and oxidation of NAD^+ by pyruvate and methylene blue, respectively, we were able to identify key molecular features necessary for the intrinsic activity of NAD^+ through kinetic analysis. Such features may explain how NAD^+ could have been selected early during the emergence of life. Simpler molecules, such as nicotinamide, that lack an anomeric carbon are incapable of accepting electrons from pyruvate. The phosphate moiety inhibits activity in the absence of metal ions but facilitates activity at physiological pH and model prebiotic conditions by recruiting catalytic Mg^{2+}. Reduction proceeds through consecutive single electron transfer events. Of the derivatives tested, including nicotinamide mononucleotide, nicotinamide riboside, 3-(aminocarbonyl)-1-(2,3-dihydroxypropyl)pyridinium, 1-methylnicotinamide, and nicotinamide, only NAD^+ and nicotinamide mononucleotide would be capable of efficiently accepting and donating electrons within a nonenzymatic electron transport chain. The data are consistent with early metabolic chemistry exploiting NAD^+ or nicotinamide mononucleotide and not simpler molecules.

Introduction

NAD^+ is found in all living organisms and is pervasive throughout central metabolism. Nicotinic acid,[1] nicotinamide,[2] and nicotinamide ribose phosphate[3] have all been shown to be synthesized under prebiotically reasonable conditions. NAD^+ is a redox active ribodinucleotide composed of an adenosine and a nicotinamide riboside held together by pyrophosphate between both 5′ positions. Since 5′-5′ linked dinucleotides easily form from activated nucleotides,[4] the prebiotic synthesis of dinucleotides, such as NAD^+, seems reasonable. The resulting NAD^+ could then be bound and exploited by prebiotic peptide or RNA catalysts.[5]

This hypothesis has led to a few conclusions that have rarely been tested. The adenosine portion of NAD^+ is frequently thought of as a "handle" that is easy for RNA and proteins to recognize and bind. Although early selections for NAD^+-binding aptamers isolated sequences that recognized the adenosine portion of NAD^+,[6] later selections identified aptamers that did not rely on the adenosine portion and instead bound the nicotinamide ring.[7] Further, synthetic efforts to manufacture more economically viable cofactors for industrial protein enzymes have identified non-adenosine containing analogues of NAD^+ that bind to natural NAD^+-enzymes and confer increased activity with respect to the natural cofactor.[8] Therefore, the adenosine portion of NAD^+ may function more as a tag for cells to distinguish between molecules for anabolism ($NADP^+$) and catabolism (NAD^+) rather than as just a useful chemical handle.[9]

If portions of NAD^+ are negligible for activity, then it is possible that the earliest redox active molecules exploited by nascent life-like chemical systems could have relied on nicotinamide alone without extra appendages. Such hypotheses are not easy to directly test with enzymes, as the active sites of proteins may alter the properties of the molecular cofactor and select for specific substrates. We recently reported on the nonenzymatic reduction of NAD^+ by α-ketoacids as a potential protometabolic reaction.[10] Here, we report on the use of this nonenzymatic reaction with derivatives of NAD^+ to probe the functional portions of the molecule (Scheme 1). The tested molecules include NAD^+, nicotinamide mononucleotide (NMN), nicotinamide riboside (NR), 3-(aminocarbonyl)-1-(2,3-dihydroxypropyl)pyridinium (DHPN or diyhydroxypropyl nicotinamide), and nicotinamide (NAM). Stability to potential prebiotic environments and the ability to nonenzymatically mediate electron transfer within an electron transport chain were tested. The data demonstrate that NAD^+ and nicotinamide

[a] L. Sebastianelli, Dr. H. Kaur, Z. Chen, Prof. S. S. Mansy
Department of Chemistry
University of Alberta
11227 Saskatchewan Drive, Edmonton T6G 2G2, Alberta, Canada
E-mail: sheref.mansy@ualberta.ca
[b] Prof. R. Krishnamurthy
Department of Chemistry
The Scripps Research Institute
10550 North Torrey Pines Road, La Jolla, CA 92037, USA

Supporting information for this article is available on the WWW under https://doi.org/10.1002/chem.202400411

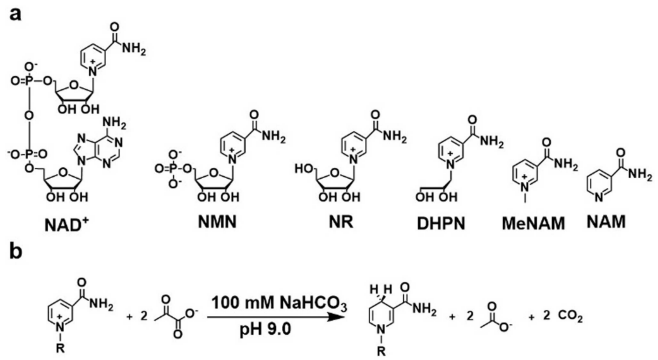

Scheme 1. a) Chemical structures of evaluated derivatives of NAD^+. b) Reaction of a nicotinamide derivative with two equivalents of pyruvate in the presence of sodium bicarbonate at pH 9.0. Nicotinamide adenine dinucleotide (NAD^+), nicotinamide mononucleotide (NMN), nicotinamide riboside (NR), 3-(aminocarbonyl)-1-(2,3-dihydroxypropyl)pyridinium (DHPN or diyhydroxypropyl nicotinamide), and nicotinamide (NAM).

mononucleotide are uniquely capable of accepting and donating electrons at pH 7.5 when Mg^{2+} is bound to their phosphate moieties. Therefore, simpler analogues of NAD^+ are unlikely to have participated in protometabolic electron transfer.

Results and Discussion

Nicotinamide is Not Sufficient for Activity

We measured the initial rates of reduction of NAD^+, nicotinamide mononucleotide, nicotinamide riboside, diyhydroxypropyl nicotinamide, methyl nicotinamide, and nicotinamide when anaerobically incubated with pyruvate at pH 9.0. Reactions were monitored by UV absorption at 340 nm (Figure S1-S5), as previously described,[10] taking advantage of the increased absorbance of the reduced pyridinium ring with respect to the oxidized pyridinium ring. Each derivative showed different reactivity with no clear correlation with steric hindrance of the redox center. Nicotinamide was completely inactive at these conditions (Figure 1). This was consistent with the inability of a pyridinium ring with a neutral tertiary cyclic nitrogen to effectively function as an electron sink. NAD^+ possesses a quaternary cyclic nitrogen with a positive charge. However, the presence of a positive charge alone (on the nitrogen) was not sufficient to generate activity similar to NAD^+. The rates of reduction of methyl nicotinamide and diyhydroxypropyl nicotinamide by pyruvate were only ca. 6% and 9% of NAD^+, respectively. Conversely, nicotinamide riboside was reduced by pyruvate at a rate 357% greater than NAD^+. This greatly increased rate suggested that the electronic effects introduced by an anomeric position were responsible for the heightened activity. The addition of a single phosphoryl group at the 5′-position of the nicotinamide riboside to generate nicotinamide mononucleotide decreased activity to 40% of NAD^+. Nicotinamide riboside was positively charged, whereas the overall charge of nicotinamide mononucleotide was negative at pH 9.0. The addition of AMP did not improve the reduction of nicotinamide mononucleotide by pyruvate (Table S1 and Figure S6). Taken together, a quaternary cyclic ammonium contributed to activity, but the dominant effect stemmed from the presence of an anomeric center within a cyclic ribo-furanose skeleton. Nicotinamide alone was insufficient for activity.

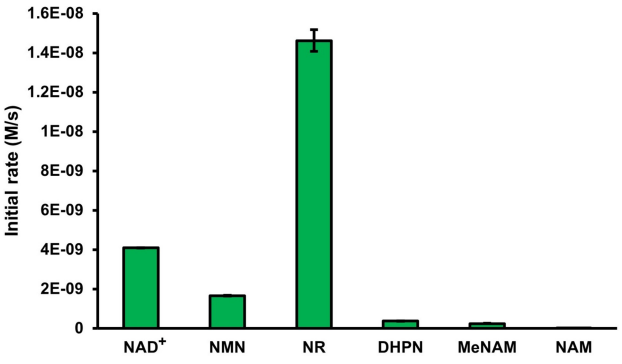

Figure 1. Initial rate of reduction with pyruvate measured during the first 4 h of the reaction. Conditions were as in scheme 1. Data are mean and standard deviation of the mean (SEM) of distinct samples, n = 3.

NAD^+ and NADH are less stable at basic and acidic pH, respectively.[11] As the nonenzymatic reactions were run at pH 9.0, we next quantified the degradation of each molecule at this pH in the absence of pyruvate (Figure S7–S8). The stability of nicotinamide and the nicotinamide derivatives directly correlated with the rate of reduction with a Pearson correlation coefficient of 0.998 (Figure 2). For example, nicotinamide riboside was reduced the most rapidly by pyruvate at pH 9.0 and was also the most rapidly degraded at the same pH in the absence of pyruvate. Analysis by LC–MS showed that degradation proceeded through the cleavage of the C–N glycosidic bond between the pyridinium ring and the sidechain. Degradation produced nicotinamide,[12] a molecule incapable of reacting

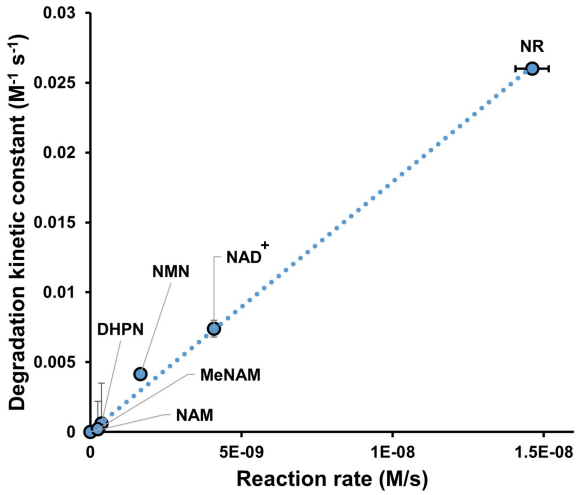

Figure 2. Correlation plot between the kinetic constants for the degradation process and the reaction rate with pyruvate. The dashed red line is the linear fit of the datapoints using $y = \rho \cdot x$, where the independent variable (x) is the reaction rate, the dependent variable (y) is the degradation kinetic constant, and the slope (ρ) is the Pearson correlation coefficient, $\rho = 0.998$. Data are mean and SEM of distinct samples, n = 3.

with pyruvate, when present. Cleavage was likely driven by nucleophilic substitution of the anomeric carbon by a hydroxide anion, releasing nicotinamide. According to this mechanism, the data points could be fit to a pseudo-first order kinetic model at constant pH giving half-lives of 26 ± 0.2 h, 94 ± 4.3 h, and 167 ± 7.1 h for nicotinamide riboside, NAD^+, and nicotinamide mononucleotide, respectively. Nicotinamide, methyl nicotinamide, and diyhydroxypropyl nicotinamide were largely stable at pH 9.0 for 24 h.

The reason for the strong correlation between degradation and reactivity towards pyruvate may have been due to coulombic effects. Both hydroxide and pyruvate are negatively charged and must interact with NAD^+ for their respective reactions to proceed. However, repulsion due to different charge densities surrounding the pyridinium ring and anomeric carbon likely inhibited the approach of hydroxide and pyruvate. This inhibition would be expected to correlate with density of negative charge. Based on this hypothesis, nicotinamide mononucleotide would experience the strongest inhibition, since the two negative charges reside on one phosphate-moiety as opposed to being spread over two phosphates in NAD^+. In fact, nicotinamide mononucleotide was reduced by pyruvate and degraded by hydroxide more slowly than NAD^+. Similarly, nicotinamide riboside, which possesses no negative charges and has a single positive charge, was reduced by pyruvate and degraded by hydroxide the most rapidly within the series. Nicotinamide, methyl nicotinamide, and diyhydroxypropyl nicotinamide lacked an anomeric carbon and thus displayed the lowest activities.

NAD^+ is Reduced by Single Electron Transfer

In contrast to mineral mediated hydride transfer,[13] we previously proposed that the nonenzymatic reduction of NAD^+ by α-ketoacids proceeded through two sequential single electron transfer (SET) steps as opposed to a single two-electron transfer (TET) event.[10] We have now modified this mechanism (Scheme S1), which still involves two sequential SET events but removes the need for an enol-form of the keto-acid as the primary initiator of the SET step. Stepwise SET reductions have been previously documented for NAD^+.[14] To confirm a SET mechanism, we used a radical trap. The logic was that a radical would be formed during the first SET step, which could be trapped by a radical scavenger. Conversely, a TET mechanism would not generate an intermediate radical and thus would be unaffected by the presence of a radical scavenger. TEMPO, i.e. (2,2,6,6-tetramethylpiperidin-1-yl)oxyl, was used as the radical scavenger. Under anaerobic conditions, 1:1:1 NAD^+:pyruvate:TEMPO in 100 mM carbonate, pH 9.0 was incubated for 24 h with stirring at 600 rpm. Subsequently, the reaction mixture was analyzed by LC–MS. Chromatograms showed the presence of non-reacted pyruvate and NAD^+, along with nicotinamide and adenosine diphosphate ribose, the products of alkaline dissociation of NAD^+ (Figure 3). No traces of NADH were found, consistent with the inhibition of a sequential SET mechanism.

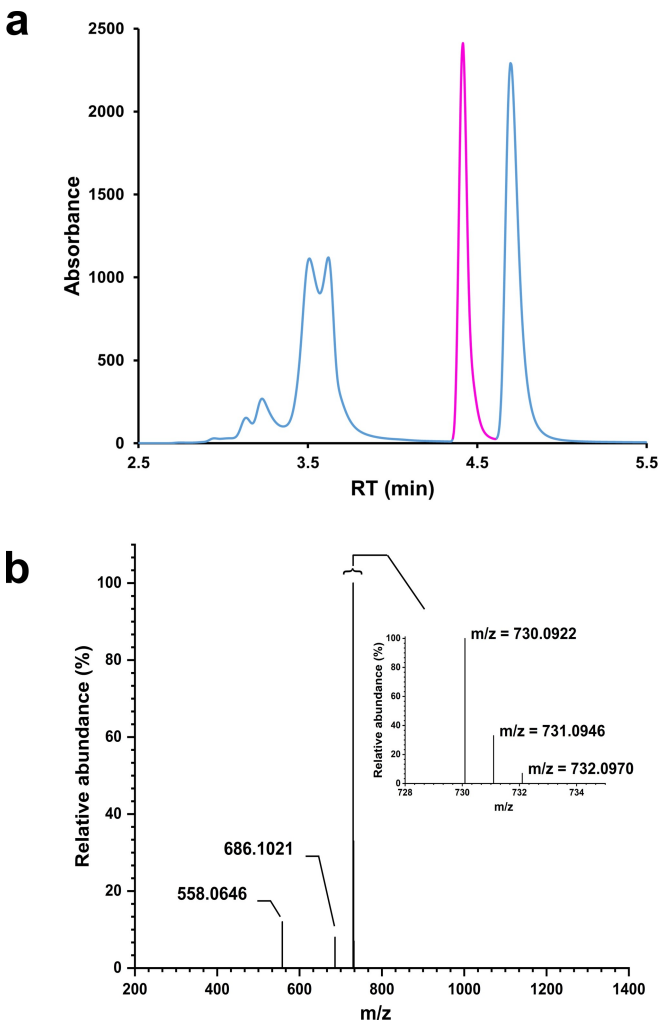

Figure 3. a) LC–MS chromatogram of the product of the reaction between NAD^+ and pyruvate in the presence of TEMPO. Retention times are pyruvate = 3.25 min, degradation products of NAD^+ = 3.55 and 3.60 min, unreacted NAD^+ RT = 4.70 min, trapped pyruvate-NAD adduct = 4.41 min (purple). b) (−)HRMS of the NAD^+-pyruvate adduct.

The chromatograms also showed the appearance of a new species with a retention time of 4.41 min (Figure 3 and Figure S9). This molecule possessed a mass-to-charge ratio of 732 and showed an absorption maximum at 370 nm, whereas the absorption maximum of NADH was 340 nm (Figure S1). The red shift of the absorption maximum was consistent with a new moiety attached to the pyridinium ring that further delocalized the aromatic pi electrons. Further high-resolution mass spectrometry (HRMS) confirmed that this new molecule was a form of a pyruvate-NAD^+ adduct, which contained a 'dehydrated' form of pyruvate bonded to the C3 of the pyridinium ring. The exact mass of the compound [M–H]- was 730.0917. The molecular formula calculated from the isotopic pattern was $C_{24}H_{27}N_7O_{16}P_2$, which differed from NADH by C_3O_2 (Figure S10). When the same reaction was repeated with the sodium salt of 2-^{13}C-pyruvate in place of unlabeled pyruvate, high-resolution mass spectrometry detected the formation of a compound with a mass [M + H] + of 733.1096, corresponding to a molecular

formula of $C_{23}{}^{13}CH_{27}N_7O_{16}P_2$ (Figure S11). The data were in agreement with a mechanism in which the reduction of NAD^+ by pyruvate was composed of two consecutive SET events, and that the intermediate collisional adduct between the two reacting molecules was a radical species that was stable enough to be intercepted by TEMPO. Such a "shutdown" of the radical mechanism by TEMPO could have caused the direct reaction of pyruvate with NAD^+ (at basic pH), giving rise to the dehydrated pyruvate-NAD^+ adduct (Figure S12), which was also supported by previous work.[15] The data were also consistent with the second of the two SET steps possessing the highest activation energy, thus functioning as the rate limiting step.

As predicted by the mechanistic pathway in Scheme S1, we probed whether the enol-tautomer of pyruvate was necessary for the nonenzymatic reduction of NAD^+ by substituting pyruvate with 3,3-dimethyl-2-oxobutyrate. This molecule is an analogue of pyruvate that does not possess an acidic proton alpha to the C2-carbonyl carbon, and therefore, cannot undergo keto-enol tautomerization. As shown in Figure S13, NADH was formed, demonstrating that the enol tautomer of an α-ketoacid was not strictly required. However, the kinetic profile of the reaction with 3,3-dimethyl-2-oxobutyrate was different from the reaction with pyruvate (Figure S1) suggesting that the sterically congested reductant may offer other pathways.

NAD^+ and NMN are Active Under Prebiotic Conditions

To determine if the nonenzymatic reduction of NAD^+ was plausible under prebiotically reasonable conditions, the reaction was measured at a few conditions that mimicked environments that may have existed on the prebiotic Earth, such as a ferrous lake, the sea, or a carbonate lake (Table S2).[16] As expected, diyhydroxypropyl nicotinamide and methyl nicotinamide were typically the least active at all these conditions (Figure 4). For the tested molecules with an anomeric carbon, the ferrous lake condition was the least conducive to activity. As the ferrous lake solutions were at pH 6.3, and the nonenzymatic reduction of NAD^+ by α-ketoacids was reported to require basic conditions,[9] the lack of activity was expected. However, the carbonate lake condition was at pH 9.0, the same pH as the reference reactions in 100 mM carbonate, and significant differences in reaction rates were observed. The nonenzymatic reduction of nicotinamide riboside fell 45-fold, whereas reactions with NAD^+ and nicotinamide mononucleotide increased 1.9- and 3.1-fold, respectively, at carbonate lake conditions in comparison to the reference reaction. Since both the carbonate lake and reference conditions were at the same pH and both contained carbonate, the observed differences likely reflected the presence of alkali and alkaline Earth metal ions in the carbonate lake conditions. Molecules with a phosphate group benefited from the presence of one or more of the metal ions present in solution (Table S2), whereas the nicotinamide riboside did not. The effect of the environment was more dramatic under seawater conditions. Here, the pH was 8.0, a value that was too low to support the nonenzymatic reduction of NAD^+ by pyruvate.[10] Nevertheless, the activity of NAD^+ and nicotinamide mononucleotide were 1.3-fold and 5.2-fold greater at seawater conditions than the reference condition at pH 9.0. The reduction of nicotinamide riboside was 8.1-fold lower. Regardless of how well the tested conditions mimicked a prebiotic environment, the seawater data suggested that metal ions allowed for reactions at lower pH than were possible under metal-free conditions.

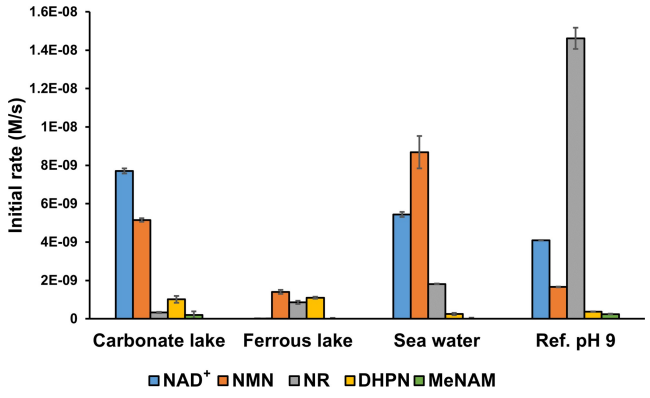

Figure 4. Initial rates of reduction with pyruvate in different environments. Ferrous lake, sea water, and carbonate lake conditions were at pH 6.3, pH 8.0, and pH 9.0, respectively. Ref. refers to the reference reaction in 100 mM carbonate, pH 9.0. Data are mean and SEM of distinct samples, n = 3.

The effect of metal ions on activity could have been to bring both reactants closer to each other. The arrangement of oxygens within pyruvate, and α-ketoacids in general, are conducive to the binding of divalent metal cations. The binding of a divalent metal cation would impart a positive charge, thus facilitating interaction with a negatively charged molecule, such as NAD^+ and nicotinamide mononucleotide. This complex would be repelled by nicotinamide riboside, which is also positively charged. Importantly, a single divalent metal ion could simultaneously bind pyruvate and the phosphate moiety of either NAD^+ or nicotinamide mononucleotide. Therefore, if the electron transfer reaction follows an inner sphere mechanism that requires a collisional adduct between pyruvate and the nicotinamide-containing molecule, as the HRMS data of TEMPO treated samples suggested, then a metal ion could facilitate this process by bringing both organic molecules within close quarters.

Phosphate Groups Recruit Catalytic Mg^{2+}

The divalent cations present in the tested environmental conditions were Mg^{2+}, Ca^{2+}, and Fe^{2+}. To determine if these metal ions impacted the rate of reduction, reactions were run at standard, reference conditions of 100 mM carbonate, pH 9.0. The influence of Zn^{2+} was also tested. Under these conditions, all the divalent cations tested increased the rate of reduction of NAD^+ by pyruvate, even at 0.03 mM divalent cation (Figure S14). However, Ca^{2+} and Zn^{2+} precipitated at higher concentrations (1–4 mM) due to complexation with carbonate. Although Fe^{2+} was more soluble, Fe^{2+} could directly reduce

NAD^+ in the absence of pyruvate under the exploited experimental conditions (Figure S15), consistent with a past report showing the binding of Fe^{2+} to NAD^+.[17] Mg^{2+} was unique in that this metal ion remained soluble at high concentrations and was not redox active.

We next evaluated how different concentrations of Mg^{2+} influenced the rate of reduction of NAD^+, nicotinamide mononucleotide, nicotinamide riboside, diyhydroxypropyl nicotinamide, and methyl nicotinamide at pH 9.0. Reduction of NAD^+ and nicotinamide mononucleotide by pyruvate showed a strong dependence on the concentration of Mg^{2+} (Figure S16). Increasing concentrations of Mg^{2+} led to increased rates of reduction with 40 mM Mg^{2+} increasing the rate of reduction 2.5-fold and 11-fold for NAD^+ and nicotinamide mononucleotide, respectively. Conversely, reaction rates were decreased for the phosphate lacking, positively charged molecules, including nicotinamide riboside, diyhydroxypropyl nicotinamide, and methyl nicotinamide (Figure S16).

To confirm that Mg^{2+} was binding to NAD^+ and nicotinamide mononucleotide and not to nicotinamide riboside, diyhydroxypropyl nicotinamide, and methyl nicotinamide, isothermal titration calorimetry (ITC) was employed. Clear endothermic peaks were observed with each addition of Mg^{2+} to NAD^+ and nicotinamide mononucleotide by ITC, whereas no clear response was observed with nicotinamide riboside, diyhydroxypropyl nicotinamide, or methyl nicotinamide (Figure S17). A one site model was used to fit the data, giving a K_d of 8.9 ± 5.5 mM for NAD^+ and 9.5 ± 7.3 mM for nicotinamide mononucleotide at pH 9.0. The data were consistent with previous reports on the binding of catalytic metal ions to the phosphate moieties of nucleotides.[18]

In light of these results, we next sought to evaluate if Mg^{2+} could rescue activity at lower pH. First, we confirmed that the rate of reduction was reduced at lower pH in the absence of Mg^{2+} (Figure S18). Reactivity at pH 7.5 was suppressed between 20- and 40-fold for each molecule in comparison to pH 9.0 (Figure S19). However, in the presence of 40 mM Mg^{2+}, the rate of reduction was partially rescued for molecules that could bind Mg^{2+} (Figure 5). For example, reaction rates increased 15-fold and 40-fold for NAD^+ and nicotinamide mononucleotide, respectively, in comparison to the same reaction in the absence of Mg^{2+} at pH 7.5. A smaller effect was observed for nicotinamide riboside (3-fold), indicating that the ring-oxygen may play a role in coordination in addition to acting as an electron-withdrawing center at the anomeric position. No activity was detected for diyhydroxypropyl nicotinamide or methyl nicotinamide either in the presence or absence of Mg^{2+}. In terms of overall yield, much less reduced product was formed at pH 7.5 after 24 h than at pH 9.0, even in the presence of Mg^{2+}. To improve detection by ^1H NMR spectroscopy, the reaction temperature was increased to 35 °C. At this higher temperature, ca. 1% of the reactants led to the formation of reduced nicotinamide mononucleotide and acetate at pH 7.5 in the presence of Mg^{2+} after 24 h (Table S1 and Figures S20-S21). For comparison, the nonenzymatic reduction of NAD^+ and nicotinamide mononucleotide by pyruvate gives rise to 3–10%[10] reduced product at pH 9.0 and room temperature

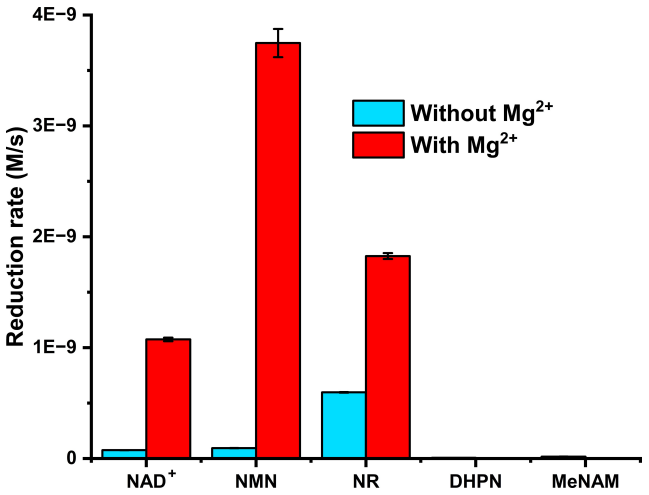

Figure 5. Initial rates of reduction of nicotinamide derivative in the absence (light blue) and presence (red) of 40 mM Mg^{2+} in 100 mM HEPES, pH 7.5. Data are mean and standard deviation of the mean (SEM) of distinct samples, n = 3.

(Table S1). To ensure that reduction could proceed with an α-ketoacid other than pyruvate, the reaction was repeated with α-ketobutyrate, which gave 4% reduced product (Table S1 and Figures S22). Taken together, the phosphate groups of NAD^+ and nicotinamide mononucleotide bind Mg^{2+} and allow for nonenzymatic reduction at physiological pH, conditions at which nucleotides are much more stable (Figure S23).[10,11]

NAD^+ and NMN are Uniquely Tuned for Oxidation and Reduction

To participate in the flux of electrons necessary to support a cell, a molecule must be capable of both accepting and donating electrons. NADH, NADPH, and BH_3CN^- display similar reactivity for donation of hydride to benzhydrylium ions.[19] We previously showed[10] that after reduction by pyruvate, NADH could subsequently donate the acquired electrons to FAD. The final electron acceptor in this chain was methylene blue. We tested the ability of the nicotinamide derivatives to participate in this nonenzymatic electron transport chain with the assumption that the interaction between FAD and methylene blue was not influenced by the type of nicotinamide derivative present (Scheme S2). The rate of depletion of oxidized methylene blue was interpreted to reflect the efficiency of the different nicotinamide derivatives in reducing FAD (Figure 6 and Figure S24). The data points were fit to a sigmoidal curve, and the rates were calculated as the slope of a line tangent to the interpolating curve at the inflection point (Figure S25-28 and Table S3).

At pH 9.0 in the absence of Mg^{2+}, there was no correlation between the rate of reduction by pyruvate and the rate of reduction of methylene blue (Figure S29). For example, the nicotinamide riboside was the most rapidly reduced by pyruvate and was the second slowest of the series in reactions leading to the reduction of methylene blue. Similarly, diyhy-

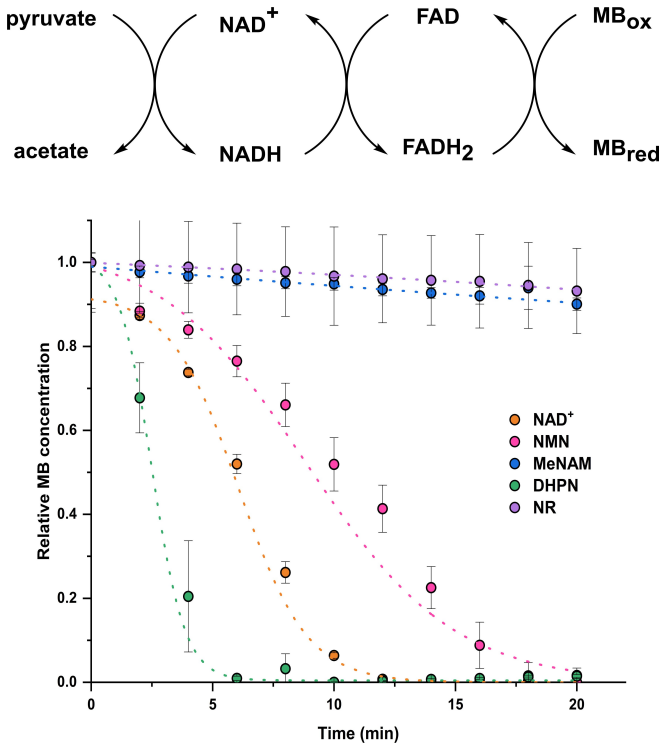

Figure 6. An electron transfer chain that mediates a flux of electrons from pyruvate to methylene blue. Oxidized methylene blue (MB) was monitored by absorption at 685 nm. Conditions were 30 mM pyruvate, 15 mM nicotinamide derivative, 7.5 mM FAD, 10 μM MB, 200 mM carbonate, pH 9.0. Data are mean and SEM of distinct samples, n = 3.

droxypropyl nicotinamide was very poorly reduced by pyruvate but was the most capable of shuttling electrons to methylene blue. The data indicated that the molecular factors influencing the reduction by pyruvate were distinct from the reduction of methylene blue through FAD.

Reducing the pH to 7.5 led to complete inhibition of the electron transport chain. The addition of 40 mM Mg^{2+} restored activity only when either NAD^+ or nicotinamide mononucleotide was present. Nicotinamide riboside was not tested because this molecule could slowly reduce oxidized methylene blue directly in the absence of FAD (Figure S30). Here again, only molecules that contained phosphate for the binding of Mg^{2+} were capable of functioning at lower pH. Although NAD^+ and nicotinamide mononucleotide were not the most rapidly reduced, both excelled at functioning as an intermediate within an electron transport chain at physiological pH in the presence of Mg^{2+} (Figure S31).

Conclusions

It remains unclear whether the earliest forms of metabolism resembled extant biology[20] or were distinct.[21] It is even less clear if protometabolism made use of an electron transport chain that coupled electron transfer with the generation of a proton gradient.[22] Nevertheless, at some point such a system emerged and must have exploited the intrinsic properties of available molecules that were then tuned by the activity of enzymes. Experiments aimed at deciphering the necessary molecular characteristics for activity are frequently difficult to probe since quantification is greatly influenced by enzymes. Our work demonstrates that nicotinamide alone is an insufficient electron acceptor, despite past assumptions. Instead, an anomeric position is required for robust activity at elevated pH, and a Mg^{2+}- binding site provided by phosphate is additionally required for activity at pH 7.5. Therefore, it seems likely that molecules such as NAD^+ and nicotinamide mononucleotide, and not simpler molecules, were exploited as starting points for RNA or peptide catalysts to regulate (proto)cellular redox chemistry. Once formed, NADH could have taken part in other prebiotic pathways, such as the synthesis of amino acids and hydroxy acids.[23]

Metabolism is a highly regulated network of reactions that ties catabolism to anabolism. To do so, most of the individual chemical steps possess high activation energy barriers that can only be traversed with the aid of an enzyme.[24] Biology frequently achieves such conditions by attaching phosphate moieties to generate molecules that are thermodynamically but not kinetically activated. Then, enzymes are deployed to catalyze the reactions when needed through an intricate relay of feedback loops.[25] Here, we find that the reduction of a prebiotically plausible molecule is kinetically inaccessible when phosphorylated in the absence of a catalyst. Conversely, in the presence of environmentally and physiologically reasonable concentrations of Mg^{2+}, the reaction proceeds, consistent with an early role for Mg^{2+}-phosphate complexes. In addition to reactivity, it is important that environmental conditions are conducive to stability. Conditions near neutrality allow for the persistence of nucleotides, including redox active nicotinamide nucleotides. The presence of Mg^{2+} protects against the degradation of amino acids[26] and is critically important for the folding and function of nucleic acids. Since model protocells have recently been identified that can grow and divide in the presence of Mg^{2+},[27] and are stable over a broad range of pH,[28] it seems that we are beginning to gain insight into which environmental conditions allow for several parts of a protocell to coexist and function. What remains challenging to decipher is how regulatory control of a supporting (proto)metabolism emerged from such chemistry.[29] The investigation of phosphorylation and Mg^{2+}-dependent catalysis may help uncover potential paths to the early appearance of feedback mechanisms that either accelerate or decelerate the kinetics of individual metabolic steps.

Experimental Section

Materials: If not specified elsewhere, all materials and chemicals were from Millipore Sigma, ThermoFisher, or APExBIO.

UV-Vis spectroscopy: Measurements were with an Agilent Cary 3500 UV-Vis Multicell Peltier instrument. Full spectra (200 nm to 1000 nm) were collected every 30 min for 17 h, unless otherwise noted.

LC–MS analysis: Chromatographic analysis exploited an Agilent LC/MSD iQ 1260 Infinity II coupled to a single quadrupole mass spectrometer. Isocratic elution was at 25 °C with 95:5 solvent A:B. Solvent A was 0.1% (v/v) ammonium formate in aqueous solution. Solvent B was acetonitrile. The reverse phase column was a Poroshell 120 SB–C18 (21.2×150 mm, 4 μm).

Reduction of nicotinamide derivatives: Each reaction was carried-out in an oxygen-free Schlenk line conditioned with at least three cycles of vacuum and nitrogen gas. Solid reagents and glass containers were similarly conditioned. Once oxygen-free, reagents were dissolved under N_2 atmosphere with Milli-Q water that was previously distilled under nitrogen. Concentrations were 100 mM carbonate, 6 mM nicotinamide derivative, and 12 mM pyruvate. The pH was adjusted with sodium hydroxide. The reaction mixture was then transferred to previously nitrogen conditioned sealed cuvettes using gas-tight syringes and monitored by UV-Vis spectroscopy. The initial reaction rates were calculated as the slope of the linear portion of plots of absorbance at 340 nm vs time. The fitting was performed with a least square method to the linear part of each curve (i.e., the first 4 to 6 h for the fastest reductions or the whole curve for the slowest cases). The conditions for radical trapping were 10 mM NAD^+, 20 mM pyruvate, 10 mM TEMPO, 100 mM carbonate, pH 9.0. Reverse phase separation was by HPLC, as described under LC–MS analysis with the following changes. The biphasic mobile phase was with eluent A (10 mM formic acid/formate, pH 3 in water) and eluent B (acetonitrile). Elution was isocratic (5% eluent B) for 0–2 min and then with a gradient between 2–10 min (from 5% eluent B to 95% eluent B). HRMS was at the Mass Spectrometry Facility of the Department of Chemistry at the University of Alberta with a ThermoScientific Orbitrap Exploris 240.

Stability: In an oxygen-free environment, each derivative was dissolved in 100 mM carbonate, pH 9.0 to a final concentration of 6 mM and left stirring continuously at 300 rpm in a sealed container. At different times, aliquots of 100 μL were removed with a gas-tight syringe and diluted with 900 μL of degassed Milli-Q water for further chromatographic analysis. Datapoints were then fit to a pseudo-first order degradation kinetic model to match the following reaction,

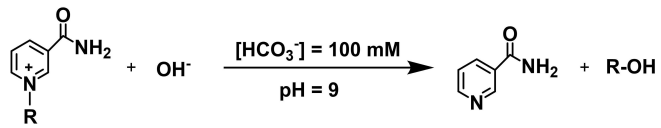

where the total concentration of hydroxide anions did not change throughout the reaction. The pseudo-first order kinetic mathematical model was

$$y = y_0 e^{-k'x}$$

where y was the concentration of the nicotinamide derivative, y_0 was the initial concentration of the nicotinamide derivative, k' was the apparent degradation constant (that included the concentration of hydroxide), and x was the time.

Electron Transport Chain: In an aerobic glovebox (Genesis 2P, Vacuum Atmospheres, $O_2 < 1$ ppm), 15 mM nicotinamide derivative, 7.5 mM FAD, and 10 μM oxidized methylene blue were dissolved in 200 mM carbonate, pH 9.0. Subsequently, pyruvate was added to a final concentration of 30 mM to initiate the electron transport chain. Reactions were monitored by following the reduction of methylene blue at 685 nm. The concentration of oxidized methylene blue through time followed a sigmoidal trend, with an initial induction time followed by a steep decrease to zero. The rate of reduction of methylene blue was calculated as the slope of the line tangent to the sigmoidal curve at the inflection point.

NMR spectroscopy: NMR spectra were recorded with an Agilent/Bruker 500 MHz spectrometer using H_2O/D_2O (80 μL DSS/D_20 + 450 μL reaction mixture) solutions at 298 K. ^1H NMR spectra (H_2O/D_2O) were solvent suppressed with presaturation. The number of scans was 8, and the delay time was 20 s. Calculation of yield was determined by using DSS (sodium trimethylsilylpropanesulfonate, 0.023 M) as an internal standard.

Pearson correlation coefficient: The coefficient was calculated with

$$r = \frac{\sum(x-\bar{x})(y-\bar{y})}{\sqrt{\sum(x-\bar{x})^2\sum(y-\bar{y})^2}}$$

where r was the coefficient, x and y were the codependent variables, and $\bar{x}$ and $\bar{y}$ were the means of the two variables.

Supporting Information

The authors have cited additional references within the Supporting Information.

Acknowledgements

We acknowledge support from the Simons Foundation (290358FY19 to S.S.M.; 327124FY19 to R.K.) and the Natural Sciences and Engineering Research Council of Canada (NSERC) [RGPIN-2020-04375 to S.S.M.]. We thank I. Betinol and T. Parkkila for preliminary experiments, and Dr. S. Basak for suggestions on experimental setup.

Conflict of Interests

The authors declare no conflict of interest.

Data Availability Statement

The data that support the findings of this study are openly available in Zenodo at https://doi.org/10.5281/zenodo.10980435, reference number 1.

Keywords: NAD^+ · prebiotic chemistry · protometabolism · nicotinamide · anomeric effect

[1] H. J. Cleaves, S. L. Miller, *J. Mol. Evol.* **2001**, *52*, 73–77.
[2] M. J. Dowler, W. D. Fuller, L. E. Orgel, R. A. Sanchez, *Science* **1970**, *169*, 1320–132.
[3] H. J. Kim, S. A. Benner, *Eur. J.* **2018**, *24*, 581–584.
[4] a) D. Puthenvedu, T. Janas, I. Majerfeld, M. Illangasekare, M. Yarus, *RNA* **2015**, *21*, 1818–1825; b) A. Mariani, D. A. Russell, T. Javelle, J. D. Sutherland, *J. Am. Chem. Soc.* **2018**, *140*, 8657–8661.
[5] a) A. C. Sanchez-Rocha, M. Makarov, L. Pravda, M. Novotný, K. Hlouchová, *eLife* **2024**, *13*, RP94174; b) J. Sileikyte, S. Sundalam, L. L. David, M. S. Cohen, *J. Am. Chem. Soc.* **2021**, *143*, 6787–6791.

[6] P. Burgstaller, M. Famulok, *Angew. Chem. Int. Ed. Engl.* **1994**, *33*, 1084–1087.
[7] C. T. Lauhon, J. W. Szostak, *J. Am. Chem. Soc.* **1995**, *117*, 1246–1257.
[8] a) T. Knaus, C. E. Paul, C. W. Levy, S. de Vries, F. G. Mutti, F. Hollmann, N. S. Scrutton, *J. Am. Chem. Soc.* **2016**, *138*, 1033–1039; b) C. E. Paul, I. W. C. E. Arends, F. Hollmann, *ACS Catal.* **2014**, *4*, 788–797.
[9] H. Kim, B. Haley, *Bioconjugate Chem.* **1991**, *2*, 142–147.
[10] S. Basak, S. Nader, S. S. Mansy, *JACS Au* **2021**, *1*, 371–374.
[11] H. K. Chenault, G. M. Whitesides, *Appl. Biochem. Biotechnol.* **1987**, *14*, 147–197.
[12] M. T. D. Campbell, D. S. Jones, G. P. Andrews, S. Li, *Food Nutr. Res.* **2019**, *63*.
[13] D. P. Henriques Pereira, J. Leethaus, T. Beyazay, A. do Nascimento Vieira, K. Kleinermanns, H. Tuysuz, W. F. Martin, M. Preiner, *FEBS J.* **2022**, *289*, 3148–3162.
[14] a) E. Ignatz, Y. Geisselbrecht, S. Kiontke, L. O. Essen, *Photochem. Photobiol.* **2018**, *94*, ; b) J. Yuasa, S. Yamada, S. Fukuzumi, *Angew. Chem. Int. Ed.* **2008**, *47*, 1068–1071; c) J. Grodkowski, P. Neta, B. W. Carlson, L. Miller, *J. Phys. Chem.* **1983**, *87*, 3135–3138.
[15] a) J. Torreilles, J. Marchand, M. C. Guerin, M. Gabriel, D. Larcher, *Biochimie* **1983**, *66*, 193–199; b) J. Marchand, J. Torreilles, M. C. Guerin, B. Descomps, A. Crastes de Paulet, M. Gabriel, D. Larcher, *Biochimie* **1982**, *64*, 203–209; c) J. Everse, E. Cooper Zoll, L. Kahan, N. O. Kaplan, *Bioorg. Chem.* **1971**, *1*, 207–233; d) A. Gafni, *Biochemistry* **1980**, *19*, 237–244.
[16] a) S. Ranjan, D. D. Sasselov, *Astrobiology* **2016**, *16*(1), 68–88; b) J. D. Toner, D. C. Catling, *Proc. Natl. Acad. Sci. USA* **2020**, *117*, 883–888.
[17] J. M. Weber, B. L. Henderson, D. E. LaRowe, A. D. Goldman, S. M. Perl, K. Billings, L. M. Barge, *Astrobiology* **2022**, *22*, 25–34.
[18] a) J. M. Lowenstein, *Biochem. J.* **1958**, *70*, 222–230; b) E. Werner, S. Pinna, R. J. Mayer, J. Moran, *J. Am. Chem. Soc.* **2023**, *145*, 21630–21637.
[19] R. J. Mayer, J. Moran, *Org. Biomol. Chem.* **2023**, *21*, 85–88.
[20] a) K. B. Muchowska, S. J. Varma, J. Moran, *Chem. Rev.* **2020**, 7708–7744; b) M. A. Keller, A. V. Turchyn, M. Ralser, *Mol. Syst. Biol.* **2014**, *10*(725).
[21] a) R. Krishnamurthy, *Chem. Eur. J.* **2018**, *63*, 16708–16715; b) M. W. Powner, J. D. Sutherland, *Philos. Trans. R. Soc. London Ser. A* **2011**, *366*, 2870–2877.
[22] C. Bonfio, E. Godino, M. Corsini, F. F. de Biani, G. Guella, S. S. Mansy, *Nat. Catal.* **2018**, *1*, 616–623.
[23] a) N. Nogal, J. Luis-Barrera, S. Vela-Gallego, F. Aguilar-Galindo, A. de la Escosura, *Org. Chem. Front.* **2024**, *11*, 1924–1932; b) R. Mayer, J. Moran, *ChemRxiv*. **2023**, doi:10.26434/chemrxiv-2023-jdhxk.
[24] S. Nader, L. Sebastianelli, S. S. Mansy, *Phil. Trans. R. Soc. A* **2022**, *380*, 20200423.
[25] a) K. Ruiz-Mirazo, C. Briones, A. de la Escosura, *Chem. Rev.* **2014**, *114*, 285–366; b) N. Nogal, M. Sanz-Sanchez, S. Vela-Gallego, K. Ruiz-Mirazo, A. de la Escosura, *Chem. Soc. Rev.* **2023**, *52*, 7359–7388.
[26] D. Rossetto, L. Valer, N. Yeh Martín, G. Guella, Y. Hongo, S. S. Mansy, *ACS Earth Space Chem* **2022**, *6*, 1221–1226.
[27] Ö. D. Toparlak, L. Sebastianelli, V. Egas Ortuno, M. Karki, J. W. Szostak, R. Krishnamurthy, S. S. Mansy, *ACS Nano* **2023**, *17*, 23772–23783.
[28] Ö. D. Toparlak, M. Karki, V. Egas Ortuno, R. Krishnamurthy, S. S. Mansy, *Small* **2020**, *16*, 1903381.
[29] N. Lauber, C. Flamm, K. Ruiz-Mirazo, *BioEssays* **2021**, *43*, 2100103.

Manuscript received: January 30, 2024
Accepted manuscript online: April 19, 2024
Version of record online: ■■, ■■

RESEARCH ARTICLE

NAD(H) and nicotinamide mononucleotide are capable of mediating model protometabolic electron transfer reactions, whereas simpler analogues are not. Early enzyme-like catalysts likely exploited molecules that possessed a nicotinamide, an anomeric position, and a Mg^{2+}-binding site, as found in nicotinamide-containing molecules in biology today.

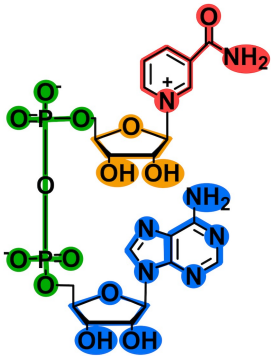

*L. Sebastianelli, Dr. H. Kaur, Z. Chen, Prof. R. Krishnamurthy, Prof. S. S. Mansy**